The Eurasia Proceedings of Science, Technology, Engineering & Mathematics (EPSTEM)
ISSN: 2602-3199

The Eurasia Proceedings of Science, Technology, Engineering and Mathematics (EPSTEM), 2025

Volume 37, Pages 131-140

ICEAT 2025: International Conference on Engineering and Advanced Technology

Service Load Behavior of Hybrid UHPC T-Beams Reinforced with GFRP Bars

Kazewa Tareq Najmaldeen
University of Kirkuk

Ali Ihsan Salahaldin
University of Kirkuk

Wael Rami Almakinachi
University of Kirkuk

Abstract: Six hybrid Tee beams reinforced with GFRP were the subject of an experimental study in this article, the main parameters that were investigated were different reinforcement ratios and different stirrup spacings. Load deflection, load-stress curve, cracking pattern behavior were all observed during the service loading stage. When compared to normal reinforcing steel bars, GFRP is known as a lightweight, non-corrosive material with a low modulus of elasticity; this property is considered the main drawback of GFRP bars. The targets of this study are to depict an experimental investigation of the flexural behavior of hybrid concrete (Ultra-high-performance concrete and normal concrete) beams reinforced with GFRP, to explore the effect of the GFRP bars on flexural capacity in terms of failure modes, serviceability, and strength. The results indicate that an increase in the reinforcement ratio leads to an enhancement in the load-carrying capacity of GFRP reinforced beams, increases the deflection, crack width, and crack distribution. Reducing the stirrups spacing increases the ductility and strength of the beams. One of the most significant findings was the decrease in the deflection by 32% when increasing the GFRP reinforcement ratio for 10 cm stirrup spacing while in on the other hand stirrup spacing of 7 cm shows a decrease in the deflection by 22% for lower percentage ratios.

Keywords: Flexural behavior, GFRP reinforcement ratio, Hybrid concrete, Interface slippage, Stirrups spacing

Introduction

Concrete is known as one of the highly used materials in construction, due to its high compressive strength and the availability of its constituents. However, concrete's limitations in withstanding tensile stresses are significant. Therefore, steel reinforcing has been used. However, as steel may be prone to corrosion, which leads to loss of strength over time, in addition to its heaviness when applied in practice, a more durable type of reinforcement has been applied in this manner. There are various methods to enhance the durability of concrete, such as working with high-performance concrete, using specific types of cement like sulfate-resistant options, conducting regular maintenance and inspections, controlling cracking, and using corrosion-resistant reinforcement (Ghaidan, Ali Ihsan, et al., 2024; Ghaidan, Mohammed, et al., 2024; Kassim & Salman, 2024; Moazzenchi & Vatani Oskouei, 2023; Selim et al., 2024). There are several kinds of fiber-reinforced polymers (FRPs), such as Carbon, Glass, Basalt, and Aramid. Due to limitations in the uses of GFRP in practice, this research evaluates the bending performance of GFRP-reinforced concrete tee beams. Comparing with standard construction materials like steel, FRP reinforcement delivers a unique combination of chemical, mechanical, and physical features, such as high stiffness-to-weight and strength-to-weight ratios, not magnetic in nature, fatigue and chemical-resistant properties, and improved corrosion resistance (Abadel, 2024; Cao et al., 2025; Issa et al., 2024; Said & Tu'ma, 2021; Salahaldin et al., 2021; Salahaldin et al., 2022).

Karabulut (2025) applied machine learning methods to estimate the flexural behavior of GFRP reinforced concrete beams, establishing a connection between the experimental results of nine RC beams and varying concrete strengths categorized as weak (C20), moderate (C30), and strong (C40) through advanced analytical methods. The study revealed that the load-capacity of the beams enhanced with the rise in compressive strength, with C40 exhibiting a 74% increase compared to C20. Conversely, the ductility behavior was more evident in concrete with lower compressive strength. Additionally, the ML models demonstrated an accuracy of 91.5% in predicting deflection values.

In a study comparing UHPC beams reinforced with BFRP and GFRP, Alhoubi et al. (2022) examined six UHPC beams. The study focused on numerous parameters, such cracking moments and patterns, failure mechanisms, deflection at midspan, and stresses in both concrete and reinforcement. In the case of lower reinforcement ratios, the UHPC beams that use BFRP bars revealed a 23% drop in flexural capacity as compared to those reinforced with GFRP bars. In contrast, the BFRP-reinforced beams exhibited a 4% improvement in flexural capacity compared to the GFRP-reinforced beams.

Najmaldeen et al. (2024) carried out a nonlinear finite element analysis using the ABAQUS program to study the behavior of eighteen T-shaped concrete beams reinforced with either steel or GFRP bars. Their work examined several influential parameters, such as the reinforcement type, different reinforcement ratios, the use of hybrid concrete with varying compressive strengths in the web and flange, and the effect of changing stirrup spacing within the shear region. The numerical results showed a substantial drop—nearly 80%—in deflection for beams reinforced with steel, whereas the GFRP-reinforced specimens exhibited an increase of about 34% in load-carrying capacity

Liu et al. (2025) conducted combined numerical and experimental research on beams reinforced with hybrid PVA fibers, aiming to enhance the stiffness of the section. Their findings indicated that incorporating PVA fibers helped reduce crack formation, improved strain distribution within the tensile zone, and contributed to an overall increase in flexural resistance.Li et al. (2024) emphasized the importance of the interaction between the concrete matrix and reinforcement under complex loading conditions. Their study assessed the flexural behavior of lightweight ultra-high-performance fiber-reinforced concrete (LUHPC) beams strengthened with high-strength steel and GFRP bars. Test results showed that GFRP-reinforced LUHPC beams (G-LUHPC) achieved higher cracking loads, peak loads, and flexural stiffness with increasing reinforcement ratios, but this improvement came at the expense of ductility. When compared with LUHPC beams reinforced with steel (S-LUHPC), the G-LUHPC specimens demonstrated reductions in bending strength of 18.2%, 24.2%, and 6.7% across the examined ratios

In the present work, the flexural response of hybrid beams composed of reactive powder concrete (RPC) in the flange and normal concrete (NC) in the web is examined, with GFRP bars used as an alternative to conventional steel reinforcement. To the authors' knowledge, the combined influence of reinforcement ratio, concrete strength variation in both the web and flange, and changes in stirrup spacing for this specific T-beam configuration has not been addressed previously. The current study investigates these parameters to better understand their collective impact on the flexural performance of hybrid T-beams

Laboratory Experiment

Material Proprieties

In this investigation normal Portland Cement (Type I) was used that met the Iraqi Standard Specifications (No. 5/2019)("Iraqi Standard Specification No.5, Portland Cement,"). During the investigation, a densified micro-silica fume with a minimum silicon-dioxide content of 85%, specific gravity of 2.3, and specific surface of 15 m^2/gram was used as a mineral additive for the RPC portion of the beams (flange). In addition, a high-performance water-reducing agent was used to improve workability at a low water-cement ratio to obtain the appropriate strength and workability for fresh concrete. Natural river sand was used as a fine aggregate with a particle size of less than 4.75mm, meeting the specification (ASTM C33/C33M-18) ("ASTM C33/C33M-18 Standard Specification for Concrete Aggregates," 2018).

As a coarse aggregate, a crushed aggregate was utilized with NMS of less than 10 mm for conventional concrete (used in the web) and met the range defined by (ASTM C33/C33M-18)("ASTM C33/C33M-18 Standard Specification for Concrete Aggregates," 2018). Table 1 shows information about concrete mix composition and compressive strength for both web and flange, which were developed to achieve the specified cubic compressive strength (F_{cu}).

Table 1. Concrete mix design

Mix	C: S	Cement (Kg/ Cu.m)	Sand (Kg/ Cu.m)	Silica fume (Kg/ Cu.m)	W/binder	HRWR Dosage% of binder	Concrete Compressive Strength, F_{cu}
Flange	1:1.35	900	1350	100	0.17	3.1%	110 MPa
Mix	C: S: G	Cement (Kg/ Cu.m)	Sand (Kg/ Cu.m)	Gravel (Kg/ Cu.m)	W/C	HRWR Dosage%	Concrete Compressive Strength, F_{cu}
Web	1:1.5:3	1000	1500	3000	0.48	0	60 MPa

The longitudinal reinforcement consisted of GFRP bars with nominal diameters of 10 mm and 12 mm, which were positioned in the tension zone of the beams. Steel bars of 8 mm diameter were used as stirrups and were also placed longitudinally at the top to secure the stirrup configuration. The mechanical properties of the reinforcement materials are listed in Table 2, while Figure 1 illustrates the tested GFRP bars

Table 2. Characteristics of GFRP

Reinforcement Type	Bar Diameter (mm)	Elastic Modulus (MPa)	Ultimate strength (MPa)
GFRP*	12	50000	1100
GFRP*	10	50000	895

*The GFRP bar was tested at Baghdad University

Figure 1. Tested GFRP bars

Details of the Beam Specimens

To perform this research, six concrete beams reinforced with GFRP were tested with varying load levels and with variable parameters such as different reinforcement ratios and stirrup spacing. Figure 2 shows the use of a simply supported Tee cross-section beam with dimensions (thickness of flange = 60 mm ,width of flange = 180 mm , depth of web = 180 mm, thickness of web= 100 mm, length of the specimen= 1600 mm). Although GFRP bars possess lower tensile strength compared to advanced fibers like CFRP, their application can still be structurally effective when integrated with high-strength concrete and properly designed cross-sections. GFRP is widely used for economical reinforcement, especially in corrosion-prone environments like marine structures and bridges.

To prevent shear failure in a shear span area, φ8 mm bar stirrups with varying spacing (7cm and 10 cm) were used for all of the tested beams; no stirrups were utilized in the beam's middle span (pure flexural region). The web was reinforced with three different reinforced ratios of GFRP (2-dia.12, dia.12+dia.10, 2-dia.10), and the flange supported the stirrups with four longitudinal φ8-mm-diameter steel bars. Hybrid concrete was used to cast the beam, which indicates that the web and flange have varying concrete compressive strengths. The web was made of normal concrete with a strength (f_{cu}) of 60 MPa.

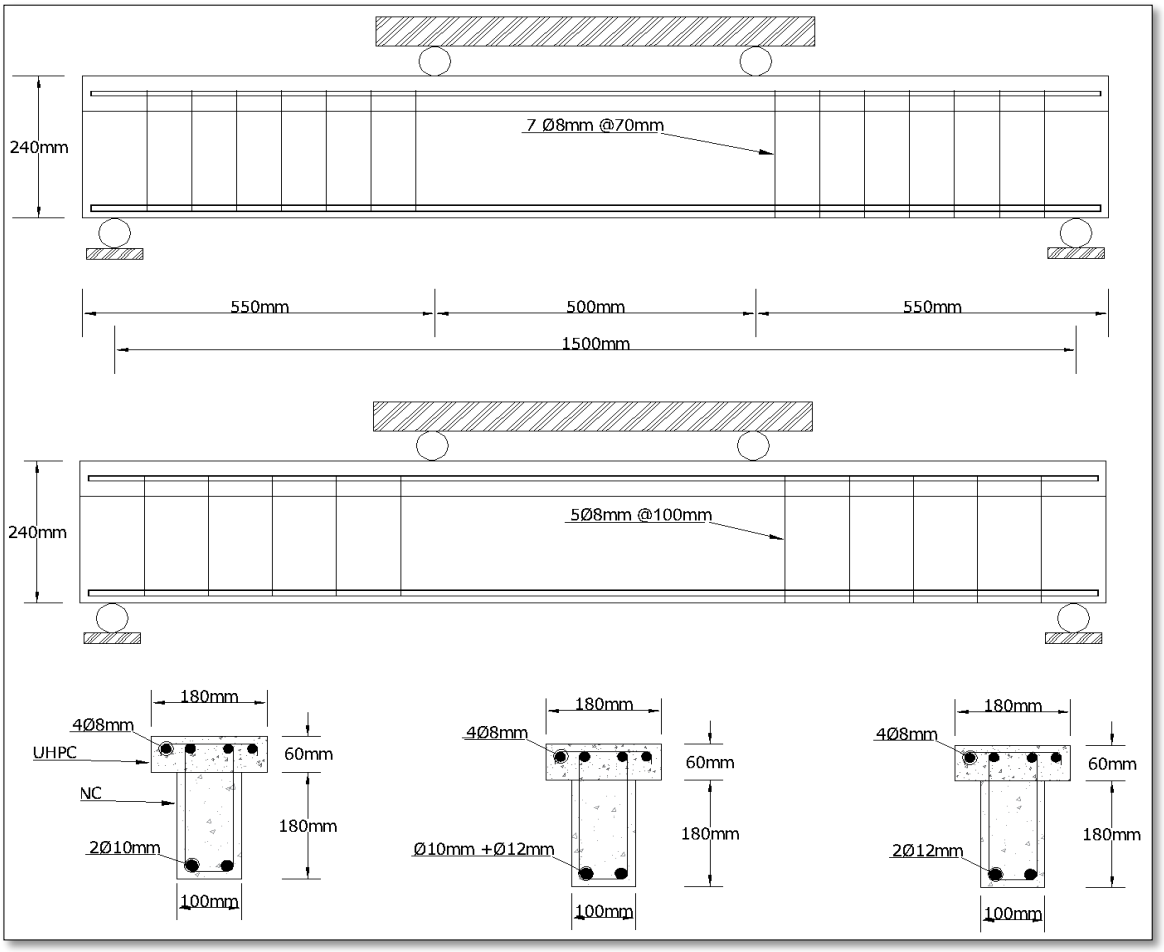

Figure 2. Reinforcement beams details (all dimensions are in mm).

The flange portion was produced using reactive powder concrete that achieved a 28-day compressive strength of 110 MPa. The construction of the hybrid T-beams was carried out in two consecutive casting stages. In the first stage, the web region was cast with normal-strength concrete and left for 24 hours to gain sufficient initial hardness. Afterward, the second stage was completed by placing the reactive powder concrete to form the flange. The mechanical and geometric characteristics of all specimens are summarized in Table 3.

Table 3. Characteristics of the tested beams.

Specimens	Type of Reinforcement	Diameter (mm)	Stirrup spacing (mm)
B200-R100	Glass fiber reinforced geopolymer	2-dia.12	100
B180-R100		dia.10+dia.12	
B160-R100		2-dia.10	
B200-R70		2-dia.12	70
B180-R70		dia.10+dia.12	
B160-R70		2-dia.10	

* (B) refers to web GFRP bars; (Numbers 200, 180, and 160) is the area made of two bars; R refers to stirrup spacing (10 and 7 cm).

Experimental Procedure

Loading Conditions and Testing

All beam specimens were tested under a two-point loading configuration while resting on simple supports. Steel I-sections were used to distribute the applied load into two symmetrical points, and steel rollers were installed at

both ends to represent pin-type supports. A linear variable displacement transducer (LVDT) with a capacity of 60 mm was positioned at mid-span to monitor deflection. Loading was applied by a 300 kN hydraulic jack in increments of 2 kN, with each step maintained for several minutes to document the development of cracking.

The nominal ultimate capacities of the GFRP-reinforced beams were estimated in accordance with The American Concrete Code (ACI 440.1R-15)("ACI 440.1R: Guide for the Design and Construction of Structural Concrete Reinforced with Fiber-Reinforced Polymer (FRP) Bars," 2015) and these theoretical limits were used as the reference for terminating the loading process. Figure 3 presents details of the test setup. All instrumentation-including the LVDT, strain gauges, and load cell—was connected to a computerized data acquisition system, allowing continuous recording of flexural crack propagation and reinforcement stresses throughout the test.

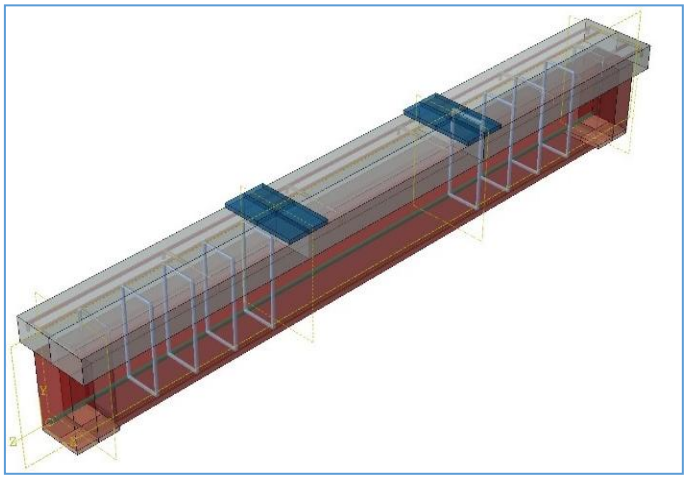

Figure 3. The beams detail

Results and Discussion

The present study aims to demonstrate experimentally how GFRP-reinforced concrete beams perform in flexural mode. The experimental result shows the load stress curve and load-deflection diagram at the service level. Results of the load with deflection are shown in Table 4. The final stage represents the end of loading, which represents the service applied load.

Table 4. Comparison of load capacity (Theoretical vs test).

Specimens	Theoretical Beam Capacity (kN)	First Crack Stage		Final Stage	
		Load (kN)	Deflection (mm)	Load (kN)	Deflection (mm)
B200-R100	145	15.57	1.14	108	43
B180-R100	106	15.22	0.94	90	40
B160-R100	94	10.3	1.68	85	36
B200-R70	145	14.63	1.21	110	38
B180-R70	106	11.55	0.94	90	35
B160-R70	94	14.21	0.94	86	28

Load-Deflection Curve

For all the GFRP-reinforced specimens, load–deflection curves were constructed to illustrate the variation in stiffness among the tested beams, as shown in Figure 4. Each curve reflects the mid-span deflection measured by the linear variable displacement transducer (LVDT) against the corresponding applied load. In general, the response of the beams can be described in two main stages. The first stage ends at the onset of cracking, where the initial change in slope appears. Beyond this point, the behavior transitions into a nearly linear phase that continues up to failure, since GFRP bars do not exhibit a distinct yield plateau. As a result, the post-cracking region remains essentially linear until the beam reaches its ultimate load.

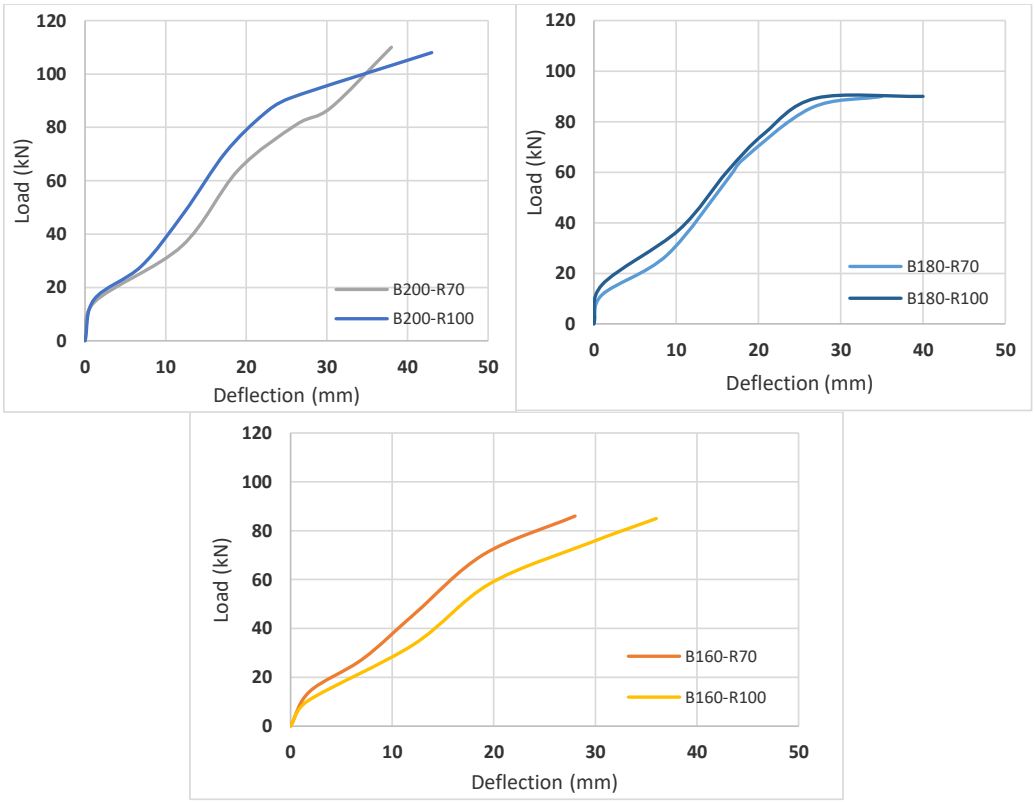

Figure 4. Load to deflection curve for the GFRP beam with different stirrup spacing.

Load-Stress Curve

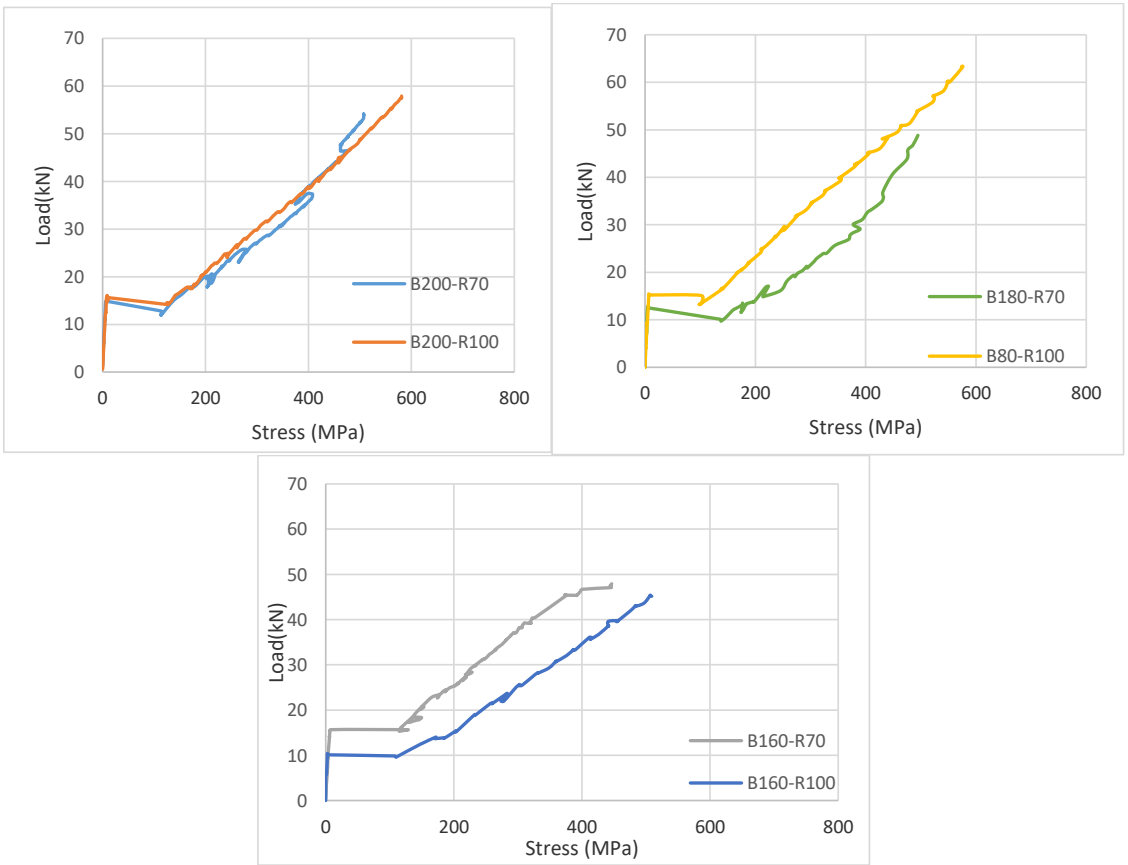

Figure 5 Load to stress curve for the GFRP beam with different stirrup spacing

Load–stress relationships were obtained at the mid-span region of each specimen, as illustrated in Figure 5. A strain gauge was fixed to the GFRP reinforcement at mid-span to record the maximum strain values, after which the corresponding stresses were determined by multiplying the measured strain by the elastic modulus of the GFRP bars (50,000 MPa). For the GFRP-reinforced beams, the resulting curves generally exhibited three distinct phases. The first phase represents the linear elastic response, during which both the concrete and the reinforcement contribute to resisting tensile stresses. Once the cracking load is reached, the slope of the curve noticeably decreases, indicating that tensile stresses are primarily transferred to the GFRP reinforcement after the formation of the first crack. In the final phase, the stress in the GFRP bars continues to rise progressively with the increasing applied load, producing an almost linear relationship up to the point of failure.

Effect of Longitudinal Reinforcement Amount and Type of Bars

The bending capacity of the concrete beams can be improved greatly by increasing the reinforcement ratio (taking into account all other fixed variables), which is the same concept that controls the flexural behaviour of steel-reinforced beams and GFRP-reinforced beams. İt can be seen that a significant increase in the bending capacity by 54% and 11% when comparing B160 with B200 and B180 beams, respectively.

Cracking Pattern

The first visible crack in the GFRP-reinforced beams generally developed near the mid-span and appeared as a vertical flexural crack at different load levels. With further loading, additional cracks formed and propagated from the support regions toward the loading points in an inclined pattern, reflecting the combined influence of bending and shear in those zones. Once each beam reached its designated service load, the test was halted before failure occurred, and the applied load was gradually released.

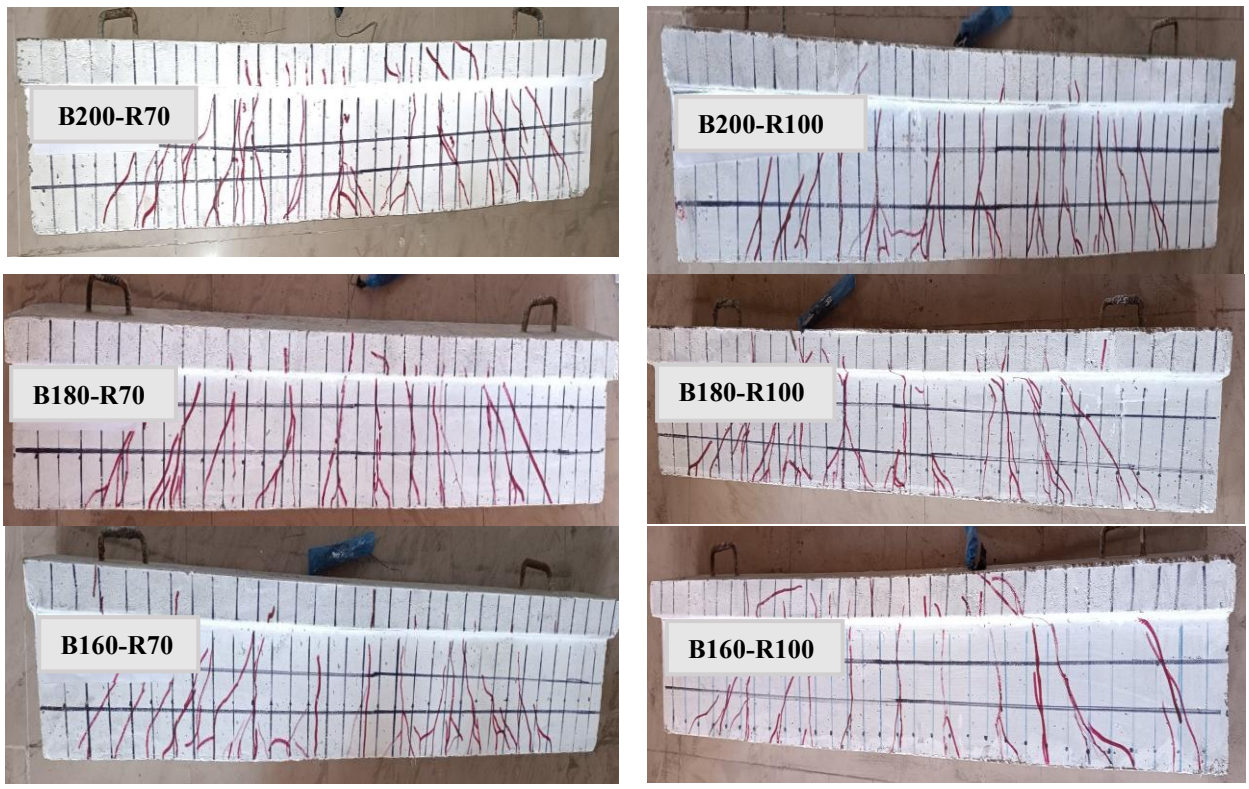

Figure 6. Crack pattern for GFRP beams

A noticeable difference in crack characteristics was observed between the two stirrup arrangements. Beams with a 10 cm stirrup spacing exhibited wider, deeper, and more widely spaced cracks compared with those reinforced at 7 cm spacing. This behavior suggests that reducing the stirrup spacing helps limit crack growth by increasing the number of intersections between the transverse reinforcement and potential crack paths, thereby enhancing the nominal shear resistance. A smaller spacing also improves the horizontal shear transfer between the RPC flange and the NC web. Figure 6 illustrates the crack patterns for the beams with both spacing configurations.

Ductility Evaluation of the Concrete T-Beams Reinforced with GFRP

Another important parameter influencing the flexural response of the beams is their ductility. In general, ductility refers to the ability of a structural member to undergo deformation beyond the elastic range while still maintaining a significant portion of its load-carrying capacity, and it is commonly expressed through a ductility index. However, this conventional definition cannot be directly applied to beams reinforced with GFRP bars, since GFRP does not exhibit a yield plateau like steel. The reinforcement remains essentially linear elastic up to failure, which limits the amount of plastic deformation that can develop. In contrast, steel reinforcement undergoes yielding and strain hardening, allowing the section to dissipate considerable inelastic energy. Because of these differences, numerous researchers have proposed alternative methods and criteria to evaluate the ductility of GFRP-reinforced concrete beams, leading to a variety of analytical approaches in the literature (Carvalho et al., 2025; Oudah & El-Hacha, 2012; Wang & Belarbi, 2011). A well-known equation was proposed early by Naaman (1995) to estimate the ductility index using an energy-based approach to calculate the FRP beam's ductility. This equation is adopted (Eq-1) to define the ductility as below

$$\mu_E = 0.5(E_t / E_e + 1) \quad \ldots (1)$$

μ_E = Ductility index for FRP reinforced beam
E_t = Total energy estimated from calculating the area under the load-deflection curve
E_e = Elastic energy estimated from calculating the area enclosed under the S line

These components are obtained through a load-deflection curve, as shown in Figure 7. The elastic slope definition, as the figure reveals, depends on choosing points S1, P1, S2, and P2. The ductility index for all GFRP reinforcing beams was calculated and is presented in Table 5. One of the most significant notes from the table is that the spacing of the stirrup influences the behaviour of the ductility of the beam. For beams B200, a decrease in the spacing of stirrups from 10 cm to 7 cm increased the ductility indices by 19%, while for beams B180, a decrease in spacing from 10 cm to 7 cm led to an increase in the ductility index by 26%. On the other hand, no difference was shown for beams B160 with respect to spacing.

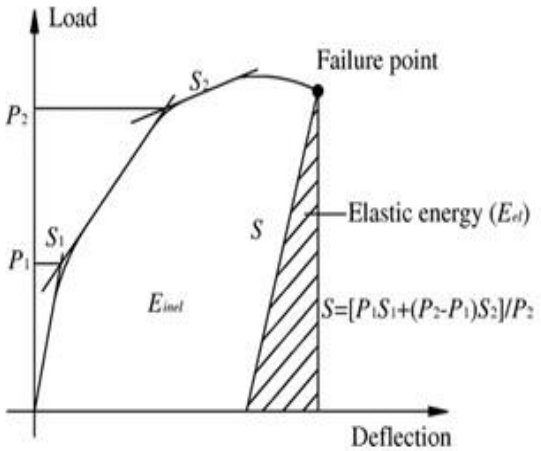

Figure 7. Energy approach definition (Naaman and Jeong, 1995)

Table 5. Ductility calculation for GFRP reinforced beams

Specimens	E_e	E_t	μ_E
B200-R100	1514.0	3045.8	1.50
B180-R100	951.6	2528.6	1.83
B160-R100	1358.7	1736.7	1.15
B200-R70	1569.0	2251.9	1.22
B180-R70	1159.0	1961.3	1.35
B160-R70	1946.1	1408.3	1.17

Conclusion

The following conclusions were drawn, which experimentally assessed the performance of the concrete T-beam reinforced with GFRP:

1. Increasing the GFRP reinforcement ratio improves the load-carrying ability, increases the bending capacity, crack width, and crack propagation of the GFRP reinforced beams.
2. Increasing the stirrups' spacing from 7cm to 10 cm for the specimens resulted in increasing midspan deflection by (13%, 14%, and 29%) at 108kN, 90kN, and 85kN, load levels, respectively, as stirrups spacing will reduce the horizontal shear flow resistance capacity between web and the flange of the concrete beams.
3. The deflection of beams with a 7 cm stirrup spacing is less than that of beams with a 10 cm stirrup spacing. In other words, increasing the transverse reinforcement ratio increases the stiffness of the beams, as it decreases the shear-flexural cracks, which was confirmed by lower deflections.
4. Reducing the spacing of the stirrup reduces the ductility of the beams (B200 and B180), while the ductility of the least reinforcement ratio beam was almost the same, as the deflection of the beams decreases as the spacing of the stirrups was reduced.
5. Increasing the stirrups' spacing from 7cm to 10 cm resulted in an increase in the stress in the bar by 9.6% and 14.6 % at load levels 53 kN,48 kN, respectively.
6. Decreasing the stirrup spacing from 10 cm to 7 cm results in an average increase of 23% in the ductility index for B200 beams, while this ratio reaches to 35% for B180 beams, with no significant difference observed for the lowest reinforcement ratio beams.

Scientific Ethics Declaration

* The authors declare that the scientific ethical and legal responsibility of this article published in EPSTEM journal belongs to the authors.

Conflict of Interest

* The authors declare that they have no conflicts of interest to report regarding the present study.

Funding

* This research received no specific grant from any funding agency in the public, commercial, or not-for-profit sectors.

Acknowledgements or Notes

* This article was presented as an oral presentation at the International Conference on Engineering and Advanced Technology (ICEAT) held in Selangor, Malaysia, on July 23-24, 2025.

References

Abadel, A. A. (2024). Flexural behaviour of RC beams with a UHPFRC top layer and hybrid reinforcement of steel and glass fiber reinforced polymer bars. *Case Studies in Construction Materials, 21*, e04017.

American Concrete Institute. (2015). *ACI 440.1R: Guide for the design and construction of structural concrete reinforced with fiber-reinforced polymer (FRP) bars*. American Concrete Institute.

Alhoubi, Y., Mahaini, Z., & Abed, F. (2022). The flexural performance of BFRP-reinforced UHPC beams compared to steel and GFRP-reinforced beams. *Sustainability, 14*(22), 15139.

American Society for Testing and Materials. (2018). *ASTM C33/C33M-18: Standard specification for concrete aggregates*. West Conshohocken, PA.

Cao, Q., Jia, Z., & Zhou, C. (2025). Flexural and serviceability behavior predictions of concrete beams reinforced with hybrid reinforcement of GFRP bars and highly ductile stainless steel bars. *Structures, 77*, 109102.

Carvalho, V. M., Campos, C. M. O., Silva, F. A., & Cardoso, D. C. T. (2025). Ductility assessment of GFRP reinforced concrete beams with a wedge-based mechanical model accounting for discrete fibers and confinement. *Engineering Structures, 322*, 119137.

Ghaidan, D., Ali Ihsan, S., & Hasan Jasim, M. (2024). Assessment of ductility indices in FRP-strengthened RC beams: A statistical analysis. *Electronic Journal of Structural Engineering, 24*(4), 8–15.

Ghaidan, D., Mohammed, H., & Salahaldin, A. (2024). Predicting failure modes of RC beams strengthening with FRP-NSM system: A statistical approach. *International Journal of Sustainable Construction Engineering and Technology, 15*, 226-240.

Issa, M., Allawi, A., & Oukaili, N. (2024). Effects of GFRP stirrup spacing on the behavior of doubly GFRP-reinforced concrete beams. *Civil Engineering Journal, 10*, 502–520.

Issa, M. A., Allawi, A. A., & Oukaili, N. (2024). Performance of doubly reinforced concrete beams with GFRP bars. *Journal of the Mechanical Behavior of Materials, 33*(1), 1-14.

Karabulut, M. (2025). Machine learning–driven flexural performance prediction and experimental investigation of glass fiber-reinforced polymer bar-reinforced concrete beams. *Polymers, 17*(6), 713.

Kassim, M. M., & Salman, G. A. (2024). The durability of concrete mortars with different mineral additives exposed to sulfate attack. *Salud, Ciencia y Tecnología – Serie de Conferencias, 3*, 851.

Li, X., Zhang, W., Zhang, C., Liu, J., Li, L., & Wang, S. (2024). Flexural behavior of GFRP and steel bars reinforced lightweight ultra-high performance fiber-reinforced concrete beams with various reinforcement ratios. *Structures, 70*, 107897.

Liu, G., Wang, B., Zhang, S., & Wang, Z. (2025). Experimental research and finite element analysis on the flexural behavior of PVA fiber concrete beam reinforced with hybrid GFRP and steel bars. *Structures, 75*, 108858.

Moazzenchi, S., & Vatani Oskouei, A. (2023). A comparative experimental study on the flexural behavior of geopolymer concrete beams reinforced with FRP bars. *Journal of Rehabilitation in Civil Engineering, 11*(1), 21–42.

Naaman, A. E., & Jeong, S. M. (1995). Structural ductility of concrete beams prestressed with FRP tendons. In *Proceedings of the 2nd International Symposium on Non-Metallic Reinforcement for Concrete Structures (FRPRCS-2)*. Ghent, Belgium.

Najmaldeen, K. T., Salahaldin, A. I., & Almakinachi, W. R. (2024). Numerical investigation of flexural behavior of hybrid concrete tee beams reinforced with GFRP. *AIP Conference Proceedings*, *3249*(1),020032.

Oudah, F., & El-Hacha, R. (2012). A new ductility model of reinforced concrete beams strengthened using fiber reinforced polymer reinforcement. *Composites Part B: Engineering, 43*(8), 3338–3347.

Said, A. I., & Tu'ma, N. H. (2021). Numerical modeling for flexural behavior of UHPC beams reinforced with steel and sand-coated CFRP bars. *IOP Conference Series: Earth and Environmental Science, 856*(1), 012003.

Salahaldin, A., Jomaa'h, M., & Naser, D. (2021). Flexural behavior of damaged lightweight reinforced concrete beams strengthened by CFRP. *Journal of Engineering Research, 9*, 1–17.

Salahaldin, A., Jomaa'h, M., Oukaili, N., & Ghaidan, D. (2022). Rehabilitation of hybrid RC-I beams with openings using CFRP sheets. *Civil Engineering Journal, 8*, 155–166.

Selim, M., Khalifa, R., Elshamy, E., & Zaghlal, M. (2024). Structural efficiency of fly-ash-based concrete beam-column joint reinforced by hybrid GFRP and steel bars. *Case Studies in Construction Materials, 20*, e02927.

Wang, H., & Belarbi, A. (2011). Ductility characteristics of fiber-reinforced-concrete beams reinforced with FRP rebars. *Construction and Building Materials, 25*(5), 2391–2401.

Author(s) Information

Kazewa Tareq Najmaldeen
University of Kirkuk, Civil Engineering Department, Kirkuk, Iraq.
Contact e-mail:*kazewatareq@gmail.com*

Ali Ihsan Salahaldin
University of Kirkuk, Civil Engineering Department, Kirkuk, Iraq.

Wael Rami Almakinachi
University of Kirkuk, Civil Engineering Department, Kirkuk, Iraq.

To cite this article:

Najmaldeen, K., T., Salahaldin, A., I. & Almakinachi, W., R. (2025). Service load behavior of hybrid UHPC T-beams reinforced with GFRP bars. *The Eurasia Proceedings of Science, Technology, Engineering and Mathematics (EPSTEM), 37,* 131-140.